

Kinetic and equilibrium studies of the biosorption of sunset yellow dye by alligator weed activated carbon

Qiang Kong^{a,b,c,1}, Qun Liu^{c,1}, Ming-Sheng Miao^c, Yu-Zhen Liu^a, Qing-Feng Chen^{d,*}, Chang-Sheng Zhao^d

^aCollege of Geography and Environment, Shandong Normal University, 88 Wenhua Donglu, Jinan 250014, Shandong, China, email: kongqiang0531@hotmail.com (Q. Kong), 75980079@qq.com (Y.-Z. Liu)

^bInstitute of Environment and Ecology, Shandong Normal University, 88 Wenhua Donglu, Jinan 250014, Shandong, China

^cCollege of Life Science, Shandong Normal University, 88 Wenhua Donglu, Jinan 250014, Shandong, China, email: 373400619@qq.com (Q. Liu), mingshengmiao@163.com (M.-S. Miao)

^dKey Laboratory for Applied Technology of Sophisticated Analytical Instruments of Shandong Province, Analysis and Test Center, Shandong Academy of Sciences, Jinan 250014, China, Tel. +86 531 82605311, Fax +86 531 82964889, email: chensdcn@163.com (Q.-F. Chen), 247898387@qq.com (C.-S. Zhao)

Received 4 May 2016; Accepted 9 September 2016

ABSTRACT

Alligator weed activated carbon (AWAC) was prepared by phosphoric acid activation. The AWAC features a high surface area (736.3 m²/g) and has an abundant array of microvoids and mesopores with an average pore size of 4.05 nm. A 0.8 g/L dose of AWAC adsorbed about 96% of sunset yellow dye (SYD) at a concentration of 150 mg/L. The maximum adsorption was approximately 271 mg/g at 308 K. Orthogonal experiments for the %Removal and amount of SYD adsorbed at equilibrium revealed that the optimal conditions were pH = 3, T = 298 K, initial SYD concentration = 250 mg/L, and AWAC dose = 1.2 g/L. The kinetics and equilibrium data agreed well with the pseudo-second-order model and Freundlich isotherm equation for the adsorbent. Functional groups that may increase the adsorption capacity were detected on the surface of AWAC, such as –OH, C=C and C–O–C. Electrostatic interactions are important in the adsorption process along with chemical bond formation and hydrophobic interaction. Thermodynamic analysis illustrated that the adsorption process is spontaneous and endothermic. AWAC is a promising low-cost adsorbent for the removal of SYD from aqueous effluent.

Keywords: Activated carbon; Adsorption; Alligator weed; Sunset yellow dye

1. Introduction

Human activities cause detrimental environmental changes that lower air, soil and water quality. In particular, water pollution endangers aquatic biota. Organic synthetic dyes are frequently used in many industrial applications including the manufacture of rubber, textiles, plastics, paper, cosmetics, pharmaceuticals and food products. The

annual production of dyes is approximately 7×10^5 tons, of which about 7×10^4 tons are discharged as waste [1,2]. Liquid wastes containing dyes are an important source of water pollution because of the obvious colors, high organic matter concentrations, and potential mutagenic and carcinogenic effects of the dyes. In addition, the discharge of dye wastewater can cause eutrophication of water bodies and may also pose a risk to human health *via* toxin enrichment in the food chain. Sunset yellow dye (SYD) is a pyrazolone dye (anionic dye) that is commonly used for food products such as can-

*Corresponding author.

¹These authors contributed equally to this work.

dies, beverages, and dairy and baked goods. Industries that manufacture these products often discharge large amount of waste containing SYD and the presence and content of SYD in effluents must be controlled [3]. It is necessary to remove high levels of dye contaminants from wastes before effluent is mixed with the natural aqueous environment.

Various management technologies have been used to remove synthetic dyes from wastewater, including physical, chemical, biological, electrochemical oxidation and adsorption methods [4]. Adsorption is the most effective and versatile method for removing pollutants like synthetic dyes, especially if there is a suitable regeneration process for the adsorbent. Biosorption has attracted the most interest because this process can remove trace amounts of synthetic dye from effluent. The use of low-cost adsorbents makes biosorption an economically viable solution for waste treatment.

Activated carbons with high specific surface areas and relatively high mechanical strength have been widely applied industrially as adsorbents in purification, as an electrode material in electrochemical devices and for separation processes [5]. Activated carbons used for dye sorption from wastewater have been prepared from low-cost agricultural byproducts including orange peel, apple pomace, banana pith, bagasse pith, cassava peel, plum kernels, wheat straw, cotton waste, teakwood bark and palm fruit bunch [6]. However, there is still need for an abundant, economical biomass and process to generate activated carbon. Alligator weed, which belongs to the Amaranth family, is a perennial plant that can be found in many aquatic and terrestrial areas of China and many other countries [7]. Alligator weed was introduced to China in 1930 and is an invasive species. Alligator weed invades agricultural areas, competes with terrestrial growth, and the decomposition of this plant causes serious pollution to water bodies [8]. Alligator weed is a hydrophyte with stems that contain airspaces, have a thin inner structure, and are rich in lignin and cellulose. Production of activated carbon from dried alligator weed is advantageous compared with other agricultural crops because it is a low-cost biomass, easy to handle, not a source of nutrients for human consumption, produces activated carbon with high surface area and efficiency for detoxifying effluents, and removal of this plant has conservational benefits [8].

Herein we investigate the potential of alligator weed activated carbon (AWAC) as a biosorbent for removal of SYD from effluent. The AWAC was characterized by various techniques such as scanning electron microscopy (SEM), surface area analyzer, porosity analyzer and Fourier transform infrared (FTIR). The adsorption capacity of the AWAC was compared with other low-cost biosorbents. The effects of various operating parameters on adsorption of SYD were monitored, such as initial concentration, contact time, sorbent dosage, temperature and pH. Moreover, the equilibrium, kinetics, isotherms, and thermodynamics of the adsorption were studied. The potential removal of synthetic dye by AWAC from waste destined for released into aquatic environments was evaluated [9].

2. Materials and methods

2.1. Chemicals

SYD (CAS# 2783-94-0) was supplied by (China) and used as received. SYD (Fig. 2a) has a molecular weight

of 452.37 g/mol and has the chemical formula $C_{16}H_{10}N_2Na_2O_7S_2$. A stock solution (1000 mg/L) of SYD in distilled water was prepared and diluted as required. All other chemicals used were analytical grade. Distilled water was used for the preparation of all solutions.

2.2. Sorbent preparation and physical characterization

Alligator weed was obtained from the Xiaoqing River in Shandong Province, China. We chose highly mesoporous alligator weed because it has large micro- and mesopores, which were expected to increase the surface area of the AWAC and increase adsorption performance. The stems were processed into lengths of 2–3 cm, cleaned with distilled water a few times to remove particulates and water-soluble impurities and then dried at 105°C in desiccators for 24 h. The dried stems were soaked in NaOH (2 wt.%) at room temperature for 24 h. The hydrolyzed stems were washed with distilled water until the pH of the filtrate was ~7 and then dried at 200°C for 1 h followed by 105°C in desiccators overnight. The material was immersed in water, phosphoric acid (1:4, g/mL) was added and the stems soaked at room temperature for 12 h. This chemical activation was expected to increase the carbon yield and develop the porous structure. Activating the material with phosphoric acid may accelerate the cleavage of bonds between cellulose and lignin and allow recombination reactions that build a rigid matrix. A rigid matrix is less prone to loss of volatiles and decreases volume contraction when heating to high temperatures [10]. The sample was transferred to a muffle furnace (Yong Guang Ming Company, Beijing, China) and carbonized at 600°C for 1 h. The resulting mass was cooled to room temperature, filtered, washed repeatedly with purified water until the pH of the filtrate was 6–7, and dried at 105°C for 12 h in desiccators. The AWAC was stored in desiccators until used in characterization and adsorption experiments [11].

The surface structure characteristics of AWAC were observed *via* scanning electron microscopy (SEM; SUPRA™ 55, Zeiss, Germany). The Brunauer–Emmett–Teller surface area and porous properties were measured from nitrogen adsorption-desorption analysis conducted at 77 K using a surface area analyzer (Quantachrome, USA). Pore size distribution and porosity were determined using a porosity analyzer (Quadrastorb SI, Quantachrome). The infrared spectrum of AWAC was recorded using a FTIR spectrometer (Thermo Scientific, USA) between wave numbers of 400 and 4000 cm^{-1} .

2.3. Adsorption equilibrium experimental studies

Batch equilibrium experiments were performed to investigate the effects of solution pH, initial concentration and temperature on SYD adsorption onto AWAC. The pH of the solution was not adjusted except for the pH effect study, where a pH range of 1–7 was investigated. The pH of solutions were determined using a pH meter and adjusted to a constant value by adding HCl (0.1 and 0.01 M) and/or NaOH (0.1 and 0.01 M). Possible loss of SYD by sorption to equipment was monitored. All experiments were conducted at room temperature except the temperature study.

For each experiment, a 100-mL stoppered conical flask containing SYD solution (50 mL, 150 mg/L) and AWAC

was mechanically agitated in a isothermal water bath shaker. Continuous mixing was maintained during the experiments with a constant agitation speed of 180 rpm to reach sorption equilibrium. The supernatant was filtered and the SYD concentration determined using a UV/visible spectrophotometer (T6-Xinshiji, Beijing, China) at a wavelength of 482 nm. The removal percentage (%Removal) and the amount of SYD adsorbed at equilibrium, (Q_e [mg/g]), were calculated using the following equations:

$$\% \text{Removal} = \left(\frac{[C_0 - C_e]}{C_0} \right) \times 100\% \quad (1)$$

$$Q_e = (C_0 - C_e) \frac{V}{W} \quad (2)$$

where C_0 and C_e (mg/L) are the initial and equilibrium concentration of the SYD, respectively; V (L) is the volume of the SYD solution; and W (g) is the mass of adsorbent used.

The effect of contact time was investigated to determine the adsorption kinetic parameters. Samples were taken at time intervals ranging from 10–360 min. The amount of SYD adsorbed (q_t [mg/g]) from initial concentrations of 150, 200 and 250 mg/L at each time point (t) was calculated by Eq. (2) using the concentration at the time points in place of C_e .

Adsorption isotherm studies were carried out with eight different initial concentrations of SYD between 100 and 300 mg/L, using 240-min contact time and an AWAC dosage of 0.8 g/L.

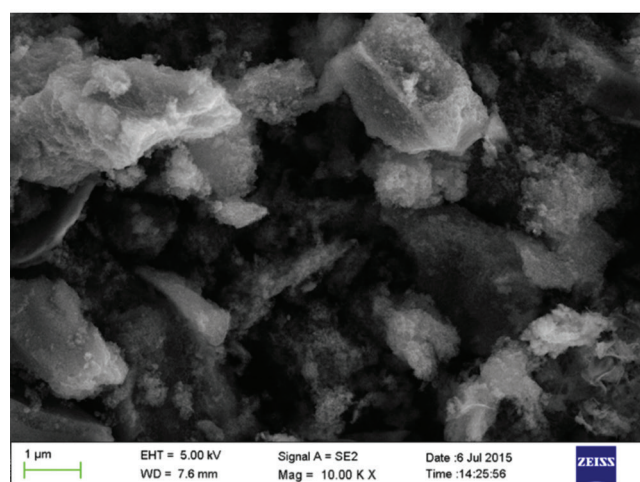
3. Results and discussion

3.1. Physical characterization of adsorbent

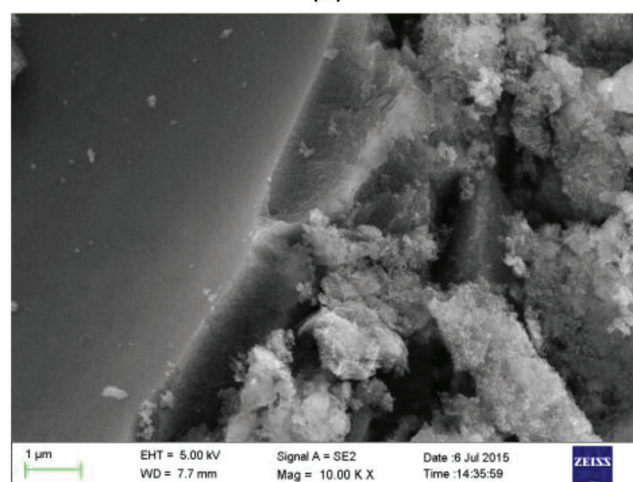
The surface morphology of the AWAC before and after adsorption were observed using SEM (Fig. 1). The surface of the AWAC before adsorption is coarse with irregular, heterogeneous porous cavities (Fig. 1a), indicating the possibility for SYD adsorption into the surface because of the high surface area and developed pore volume. The numerous large pores were filled with adsorbate after exposure to SYD (Fig. 1b), decreasing the number and volume of the pores.

The shape of the N_2 -adsorption isotherms indicates a mixture of type I and IV behavior (data not shown). A wide hysteresis loop at high relative pressures indicates a mixture of micropores and mesopores on the AWAC surface. Micropores and small mesopores were observed on the AWAC and have an average pore width of 4.05 nm, but macropores were not present. This pore distribution should enhance the adsorption capacity AWAC for small molecules [12] and be large enough to allow high adsorption capacity of large adsorbate molecules. The calculated Brunauer–Emmett–Teller surface area of AWAC is 736.3 m^2/g , which is higher than that of activated carbon derived from rice husk (480 m^2/g) [13] and slightly less than that of luffa sponge activated carbon (810.12 m^2/g) [11]. The AWAC prepared is likely to have outstanding adsorption performance.

The FTIR spectra of the AWAC before and after the adsorption process are presented in Fig. 2. The broad band at 3500 cm^{-1} is attributed to the stretching vibration of the



(a)



(b)

Fig. 1. SEM images of AWAC before (a) and after SYD adsorption (b).

–OH groups. The decreased in transmittance after treatment with SYD may be because of adsorbate ions interacting with the –OH functional groups of the AWAC. Angular deformation of the band at 1623 cm^{-1} is observed, and the intensity of the deformation depends on anionic interaction with an adsorbent [4]. The peak at 1602 cm^{-1} corresponds to the C=C stretch-vibration of aromatic rings [14]. The bands at 1164 and 1175 cm^{-1} are likely because of C–O–C functional group vibrations. The intensity of the peaks at 496 and 1576 cm^{-1} were slightly lower after adsorption of SYD to AWAC, indicating that the AWAC surface functional groups were covered or interacting with the SYD. The peaks around 1400 and 880 cm^{-1} are ascribed to the m^2 -mode of CO_2 adsorbed from air [15] and are decreased by displacement by SYD. The band at 496 cm^{-1} is mainly attributed to M–O lattice vibrations (M–OH, M–O–M or O–M–O), which decreased after adsorption of the SYD in the water [16]. The new peak at 982 cm^{-1} after adsorption might be caused by bound SYD ions.

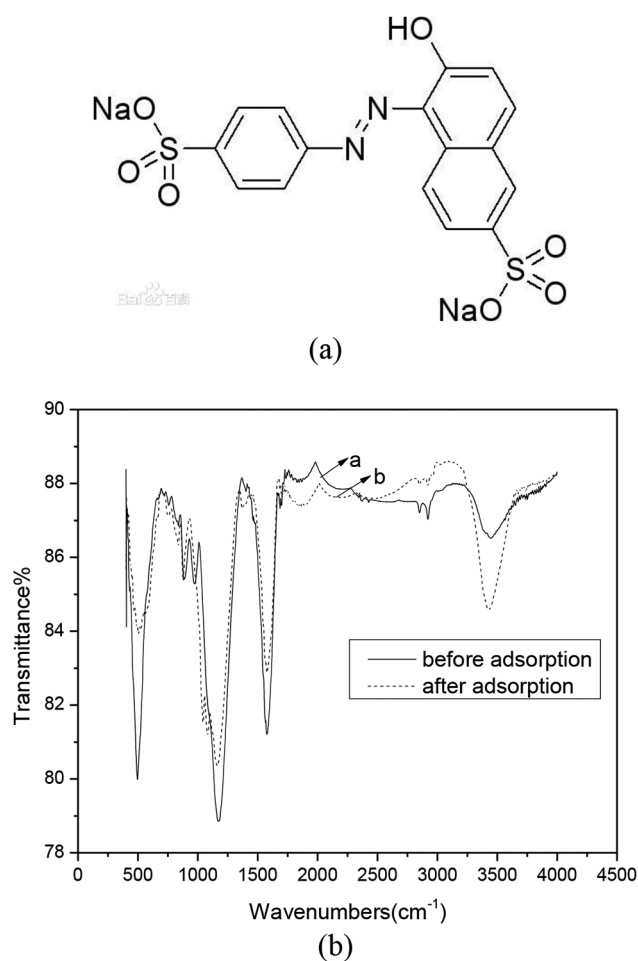


Fig. 2. Molecular structure of SYD (a) and FTIR spectra of the AWAC before and after SYD adsorption (b).

3.2. Effect of adsorbent dose on SYD adsorption

The adsorbent dose has a great effect on the adsorptive %Removal of SYD and equilibrium capacity of the AWAC. The %Removal has a first-order dependence on adsorbent dosage, and reached ~90% of the maximum amount at an AWAC dosage of 0.8 g/L (Fig. 3). The equilibrium adsorption capacity declined linearly with the AWAC dosage. The trends deviated from linearity at low dosages because of saturation of the available surface sites. Repulsive forces between the solvated SYD molecules caused no notable difference in the adsorption capacity of SYD on AWAC [17]. We chose an AWAC dosage of 0.8 g/L for subsequent equilibrium experiments for optimizing the adsorption of SYD.

3.3. Effect of initial concentration and agitation time on adsorption

The experimental constant time is defined as the time period required for the AWAC and SYD molecules reached the equilibrium adsorption before filtering. Differences in the constant time caused by experimental variables reveal the transfer rate between the adsorbent and adsorbate [18].

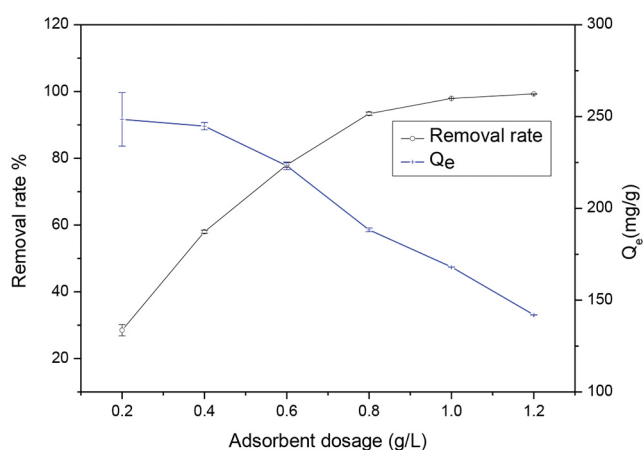


Fig. 3. Effect of AWAC dose on removal rate and adsorption capacity (initial SYD concentration 150 mg/L, adsorbent dosage 0.8 g/L, temperature 25°C time 4 h and initial pH).

The effect of agitation time on the removal of SYD at initial concentrations of 150, 200 and 250 mg/L by AWAC was investigated (Fig. 4). The adsorption rate was rapid for the first 10 min because of the presence of numerous vacant adsorption sites at the early stages of the process. Uptake became almost constant after agitating for 240 min for all concentrations, and this could be because of limited vacant sites and repulsive forces among the solvated molecules. The constant uptake indicates that the surface adsorption equilibrium was reached and that solute molecules began to enter the pores of the AWAC and were adsorbed by the interior of the particles. An optimal agitation time of 240 min was used in subsequent adsorption experiments. The equilibrium adsorption capacity accreted with increasing initial concentration and may be attributed to the increase amounts of SYD molecules competing for the available binding sites on the surface of the AWAC [19].

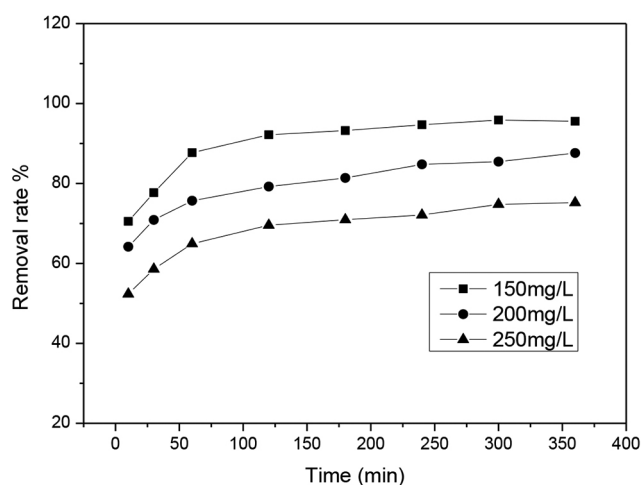


Fig. 4. Effect of contact time on the adsorption of SYD by selected adsorbents (initial SYD concentration are 150, 200, and 250 mg/L, adsorbent dosage 0.8 g/L, temperature 25°C and initial pH).

3.4. Effect of solution pH on SYD adsorption

The effect of solution pH on the adsorptive removal of SYD was studied in the pH range of 1–7 at an initial SYD concentration of 250 mg/L (Fig. 5). At pH greater than 7 SYD changes color to red, interfering with the colorimetric analysis. The highest adsorption of SYD on AWAC occurred at pH 1. The removal efficiency decreased markedly as the pH increased from 2 to 6 and then remained almost constant between pH 6 and 7 (Fig. 5). The percentage of dye removal will increase for anionic dye adsorption at low pH because the positive charge on the solution interface will increase and attract the anionic dye [20]. The adsorption was maximal at pH 1, where the removal rate reached 95%. It seems that dye removal decreased with increasing pH from 2–6 because the adsorption of SYD on AWAC occur *via* interaction with surface functional groups. The %Removal decreased as the pH was increased and is attribute to SYD adsorption occurring through electrostatic interaction or hydrogen bonding with the various groups of adsorbent [3]. Electrostatic interactions are important in the adsorption process along with chemical bonding formation and hydrophobic interaction [21]. For further optimization we chose to leave the pH of the SYD solution unadjusted (pH = 6.92).

The point of zero charge (pHpzc) is the most important parameters in the pH study of adsorbents. The pHpzc indicates the influence of pH on adsorbent chemical characteristics and adsorption capacity. The pHpzc was determined by preparing SYD solutions with initial pH values ($\text{pH}_{\text{initial}}$) ranging from 1–7, mixing with AWAC until the equilibrium adsorption time, and measuring the final pH (pH_{final}). The difference in pH_{final} and $\text{pH}_{\text{initial}}$ was plotted against $\text{pH}_{\text{initial}}$ and the pHpzc is the point where $\text{pH}_{\text{initial}} = \text{pH}_{\text{final}}$. The pHpzc for the AWAC was found to be about 3.6. The maximum adsorption capacity of SYD was at pH 1 because anionic dye adsorption is favored at $\text{pH} < \text{pHpzc}$ where the surface becomes positively charged [22].

3.5. Effect of solution temperature on SYD adsorption

The AWAC sorption of SYD at a concentration of 150 mg/L increased with temperature from 283 to 313 K (Fig. 6).

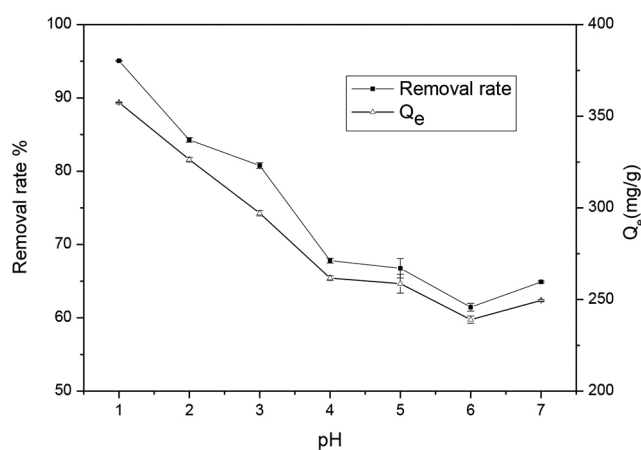


Fig. 5. Effect of solution pH on sunset yellow dye removal rate and adsorption capacity (initial sunset yellow dye concentration 250 mg/L, adsorbent dosage 0.8 g/L, time 4 h and temperature 25°C).

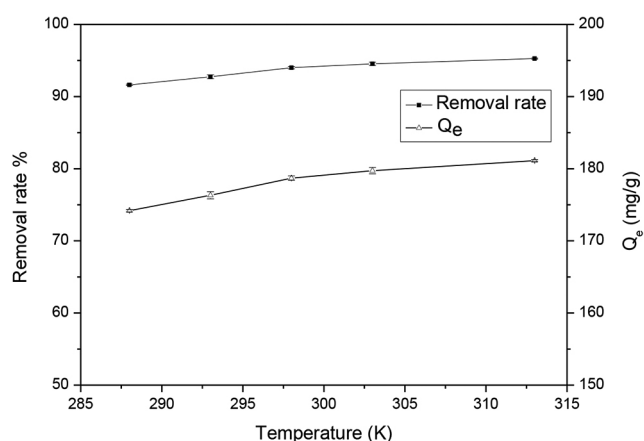


Fig. 6. Effect of temperature on removal rate and adsorption amount (initial SYD concentration 150 mg/L, adsorbent dosage 0.8g/L, time 4 h and initial pH).

The %Removal and equilibrium adsorption capacity also increased slightly from 91% to 95% and 175 to 181 mg/g, respectively. SYD removal percentage and adsorption capacity increased with increasing temperature, showing endothermic adsorption. This result supports ionic bonding between SYD and AWAC [23]. However, the temperature effect was negligible. All further experiments were carried out at 25°C.

3.6. Adsorption kinetic studies

Understanding the adsorption kinetics allows efficient process design and control of the equilibrium time. The mechanism of SYD adsorption was explored by comparing the kinetic experimental data with pseudo-first-order, pseudo-second-order, and intraparticle diffusion models.

We used an established pseudo-second-order kinetic equation [24]:

$$\ln(Q_e - Q_t) = \ln Q_e - k_1 t \quad (3)$$

where Q_e (mg/g) and Q_t (mg/g) are the amounts of SYD adsorbed at equilibrium and at time t (min), respectively, and k_1 (1/min) is the rate constant. The k_1 value is determined by the slope of a plot of $\ln(Q_e - Q_t)$ versus t .

The pseudo-second-order kinetic equations used are [24]:

$$\frac{t}{Q_t} = \frac{1}{k_2 Q_e^2} + \frac{t}{Q_e} \quad (4)$$

$$\frac{t}{Q_t} = \frac{1}{V_0} + \frac{t}{Q_e} \quad (5)$$

where k_2 (g/[mg min]) is the rate constant and V_0 (mg/[g min]) represents the initial sorption rate. The linear plot of t/Q_t versus t gives a slope of $1/Q_e$ and an intercept of $1/k_2 Q_e^2$.

The following intraparticle diffusion model was used [25]:

$$Q_e = k_p t^{0.5} + C \quad (6)$$

where k_p (mg/[g min^{0.5}]) is the intraparticle diffusion rate constant, which can indicate the rate of the adsorption process. C (mg/g) is proportional to the extent of the boundary layer thickness. k_p and C can be obtained from a plot of Q_e versus $t^{0.5}$. Intraparticle diffusion is considered the rate-limiting step if a plot of Q_e versus $t^{0.5}$ is a straight line that passes through the origin.

The correlation coefficients (R^2) of both the pseudo-first-order and pseudo-second-order models are reasonably good ($R^2 > 0.95$) for the three concentrations of SYD solution studied (Table 1). The best fit for the data was from the pseudo-second-order model where R^2 values were 0.9999, 0.9994, and 0.9992 for initial SYD solution concentrations of 150, 200, and 250 mg/L, respectively. Additionally, the calculated Q_e values from the pseudo-second-order model are in close agreement with the experimental data. The presence of a second-order sorption kinetics indicates that the process is controlled by chemisorptions.

The adsorption data for all SYD concentrations exhibit multi-linear plots, indicating that two steps influence the adsorption process (Fig. 7). The first process is the rapid adsorption to the external surface. The second process is a gradual adsorption stage ascribed to rate-limited intraparticle diffusion [25].

The C and k_p values of the two stages for the three different concentrations of SYD are shown in Table 1. The C value increased and the k_p value decreased with time during the adsorption process, showing that intraparticle diffusion has a considerable influence on the rate of adsorption at the later stage of the process.

3.7. Adsorption isotherms

The adsorption isotherm model is critical for describing how the adsorption molecules distribute between the liquid and solid phase during the adsorption process. Equilibrium data, which are commonly known as adsorption isotherms, are important for predicting the adsorption capacity and describing the surface characteristics and affinity of the adsorbent. We used three isotherm models (Langmuir, Freundlich and Dubinin–Radushkevich) to describe the equilibrium data for the adsorption of SYD onto AWAC.

The Langmuir isotherm is a monolayer adsorption processes that assumes homogeneous adsorbent structure, where all sorption sites are energetically identical [26]. The linear form of the Langmuir isotherm equation is given as:

$$\frac{C_e}{Q_e} = \frac{1}{Q_m k_L} + \frac{C_e}{Q_m} \quad (7)$$

where Q_m (mg/g) is the maximum SYD adsorption capacity and k_L (L/mg) is the Langmuir constant that is related to the energy (of adsorption).

A dimensionless constant separation factor or equilibrium parameter is defined according to the following equation to explore whether the adsorption process is favorable or unfavorable [27]:

$$R_L = \frac{1}{(1 + k_L C_0)} \quad (8)$$

where the value of R_L indicates the isotherm to be favorable ($0 < R_L < 1$), unfavorable ($R_L > 1$), linear ($R_L = 1$) or irreversible ($R_L = 0$).

The Freundlich isotherm is based on the assumption that the adsorption process occurs on a heterogeneous surface through a multilayer adsorption mechanism. The Freundlich equation can be written in the following manner [28]:

$$\ln Q_e = \ln k_F + \ln \frac{C_e}{n} \quad (9)$$

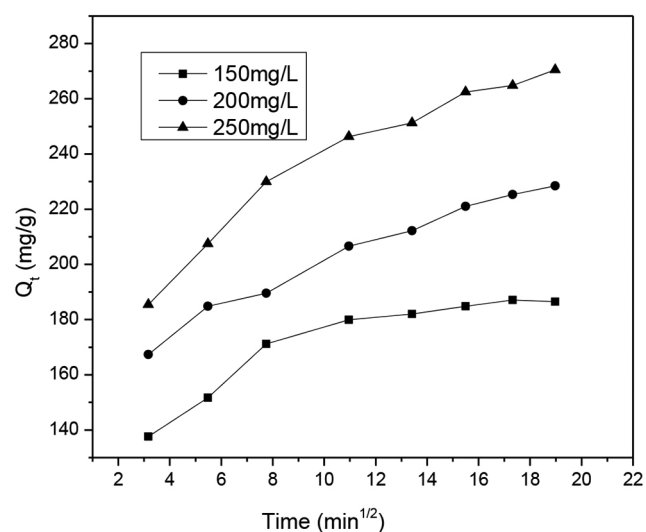


Fig. 7. Plot of intraparticle diffusion model for adsorption of SYD adsorbed onto AWAC (initial SYD concentration are 150, 200, and 250 mg/L, adsorbent dosage 0.8 g/L, temperature 25°C and initial pH).

Table 1

Pseudo-first-order, pseudo-second-order and particle diffusion models for the adsorption of SYD by AWAC

Concentration (mg/L)	Exp-data Q_e (mg/g)	Pseudo-first-order kinetics			Pseudo-second-order kinetics				Particle diffusion model		
		K_1 (min ⁻¹)	Q_e (mg/g)	R^2	K_2 (g.mg ⁻¹ .g ⁻¹)	Q_e (mg/g)	V_0 (mg.g ⁻¹ .min ⁻¹)	R^2	K_p (mg.g ⁻¹ .min ^{-1/2})	C (mg/g)	R^2
150	185	0.0170	48	0.9636	0.00086	189	30.58	0.9999	1.3544	162.98	0.9074
200	221	0.0104	55	0.9852	0.00023	238	12.89	0.9994	3.6606	164.10	0.9636
250	262	0.0244	69	0.9989	0.00041	270	29.76	0.9992	4.7674	188.08	0.9589

where k_F is the Freundlich constant and $1/n$ is a constant that relates to the intensity of adsorption or surface heterogeneity ($1/n \approx 0$ indicates that the surface is more heterogeneous and $1/n < 1$ indicates favorable adsorption).

The Dubinin–Radushkevich model can be expressed as follows [28]:

$$\ln Q_e = \ln Q_m - \beta \varepsilon^2 \tag{10}$$

$$\varepsilon = RT \ln \left(1 + \frac{1}{C_e} \right) \tag{11}$$

$$E = \frac{1}{(2\beta)^{1/2}} \tag{12}$$

where β (kJ^2/mol^2) is the adsorption energy constant; ε is the Polanyi potential; R is the thermodynamic constant; and E (kJ/mol) is the average free energy of adsorption. The values of β and Q_m can be found from the intercept and slope of the fitted line, allowing the calculation of E .

The Langmuir, Freundlich and Dubinin–Radushkevich model data are compared with the experimental data of SYD adsorption at 25°C in Fig. 8. The isotherm constants and correlation coefficients obtained for the isotherm models are summarized in Table 2. Both the Langmuir and Freundlich isotherm models provided a good fit with the experimen-

tal data ($R^2 > 95$), with better agreement from the Langmuir equation (R^2 values > 0.98). The Langmuir model is suitable for describing the adsorption interaction as monolayer coverage of SYD onto AWAC particles. In addition, this model accurately predicted the maximum SYD adsorption capacity of AWAC as 271 mg/g at 308 K ($R^2 = 0.9899$). The values of $1/n$ were less than 1 for the Freundlich model, suggesting that the adsorption is a favorable process. The Dubinin–Radushkevich model does not accurately describe the adsorption process and predicted Q_m values that were considerably different to the experimental data resulting in the low R^2 values (< 0.95). Comparing the adsorption capacity of AWAC with other low-cost AC adsorbents (Table 3) [29–31] shows that alligator weed is a good potential adsorbent material source for SYD removal from effluent.

3.8. Adsorption thermodynamics

Entropy change is the driving force of adsorption. Adsorption experiments were conducted at different temperatures in the range of 288–308 K to explore the adsorption mechanism and determine the thermodynamic parameters.

$$\ln K_L = \frac{\Delta S^\circ}{R} - \frac{\Delta H^\circ}{RT} \tag{13}$$

$$\Delta G^\circ = -RT \ln K_L \tag{14}$$

$$\Delta G^\circ = \Delta H^\circ - T\Delta S^\circ \tag{15}$$

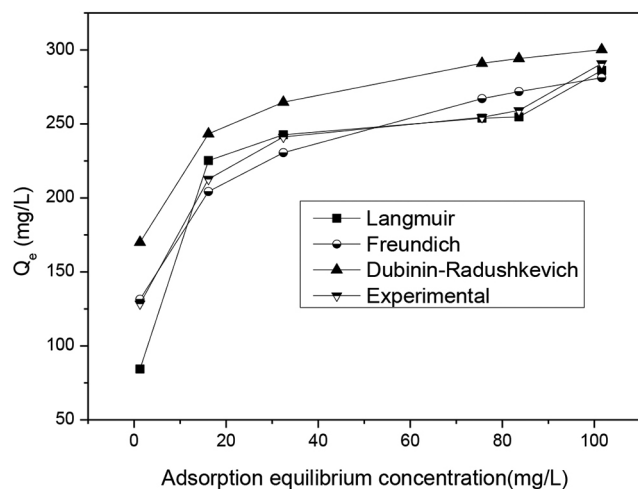


Fig. 8. Comparison of experimental data with models at 298 K.

where R ($8.314 \text{ J}/(\text{mol K})$) is the universal gas constant; T (K) is the absolute temperature of the solution; ΔG° is the standard Gibbs free energy change; ΔH° is the enthalpy change; and ΔS° is the entropy change. The values of ΔH° and ΔS° can be determined by the slope and intercept of the plot of $\ln K_L$ versus $1/T$. These parameters can be used to determine the feasibility and nature of the adsorption process [32].

The calculated thermodynamic parameter values for the sorption process are reported in Table 4. Negative ΔG° values were calculated for all temperatures, indicating that the adsorption process was spontaneous for the temperature range studied. We note that the change in free energy increased with temperature and this may be because the rate of adsorption accelerates at elevated temperature. The calculated ΔG° at 288, 298 and 308 K agree with the Langmuir equation data, which predicted adsorption capacity increases with temperature. The positive value of ΔH° indicates the endothermic nature of adsorption

Table 2

Adsorption isotherms of Langmuir, Freundlich, Dubinin–Radushkevich models and correlation coefficients for adsorption of SYD onto AWAC

Temperature (K)	Langmuir model			Freundlich model			Dubinin–Radushkevich model			
	Q_m (mg/g)	K_L (L/mg)	R^2	$1/n$	K_f (mg/g) $^{1/n}$	R^2	B (mol 2 /J 2)	Q_m (mg/g)	E (kJ/mol)	R^2
288	132	0.1845	0.9919	0.1508	64.1613	0.9566	2×10^{-9}	329	15811	0.9280
298	263	0.3689	0.9992	0.1738	125.9519	0.9763	1×10^{-9}	463	22361	0.8762
308	271	0.2960	0.9899	0.1747	132.3169	0.9661	1×10^{-9}	713	22361	0.8904

Table 3
Adsorption capacities of various low-cost AC adsorbents for SYD

Absorbent	Q_m (mg/g)	Dosage (g/L)	pH	Concentration (mg/L)	Source
CdTN-AC	181.81	2×10^{-5}	1	150	[38]
Cd(OH) ₂ -NW-AC	76.9	1	1	60	[39]
(Ag-NP)-AC	37.03	1	1	60	[39]
ZnO-NPs-AC	142.85	0.015	2	40	[40]
AWAC	271	0.8	Initial	250	This work

Table 4
Thermodynamic parameters for the adsorption of SYD onto AWAC

T (K)	K (L/mol)	ΔG (kJ/mol)	ΔS (J/mol K)	ΔH (kJ/mol)
288	69122.4	-26.68		
298	129153.4	-29.16	180	25
308	135642.3	-30.26		

interaction. Additionally, a positive value of ΔS° revealed an increase in disorder at the solid–solution interface after adsorption of SYD on AWAC [33].

3.9. Orthogonal experiments

Orthogonal experiment design and analysis is the most common method for experimental analysis. An orthogonal test can be designed based on a number of variable factors that affect experimental outcomes [34]. We used four factors and three levels in our orthogonal test method. Range analysis was used to study the order of the effect on the %Removal and equilibrium adsorption amount of the four factors. The four factors investigated were dosage of AWAC, initial concentration of SYD solution, contact time, and temperature.

The orthogonal tests were designed from the initial single-factor experiments, and the results are presented in Table 5. From these experiments we found that optimal conditions for adsorption of SYD by AWAC were at pH = 3, T = 298 K, initial SYD concentration = 250 mg/L, and AWAC content = 1.2 g/L based on maximizing the criteria of %Removal and amount of SYD removed at equilibrium. Range analysis of the orthogonal experiments (Table 6) showed the order of importance of the four factors on removal efficiency are dosage of AWAC > solution pH > concentration of SYD > temperature. The adsorption capacity order of importance was concentration of SYD > dosage of AWAC > solution pH > temperature. The influence

Table 5
Orthogonal experiment results for the adsorption of SYD on AWAC

S.No.	pH	Temperature (T)	Concentration (mg/L)	Dosage (g/L)	Removal rate (%)	Equilibrium amount (mg/g)
1	1	288	250	0.8	94.48	327.13
2	2	288	150	0.4	68.59	141.48
3	3	288	200	1.2	99.11	293.63
4	2	298	200	0.4	61.29	181.58
5	3	298	250	1.2	96.03	332.5
6	1	298	150	0.8	99.59	205.41
7	3	308	150	1.2	99.47	205.16
8	1	308	200	0.4	71.08	210.56
9	2	308	250	0.8	83.51	289.14

Table 6
Range analysis of orthogonal experiments

Level	pH	Temperature (mg/L)	Concentration (K)	Dosage (g/L)
K1	265.15	262.18	267.65	200.96
K2	213.39	259.91	231.48	277.58
K3	294.61	254.06	274.02	294.61
Adsorption efficiency				
K1	88.38	87.39	89.22	66.99
K2	71.13	85.64	77.16	92.53
K3	98.05	84.69	91.34	98.20
R	26.92	2.7	14.18	31.21
K1	743.07	762.64	552.02	533.62
Adsorption capacity				
K2	612.2	719.49	685.77	821.68
K3	831.29	704.86	948.77	831.29
K1	247.69	254.08	184.01	177.87
K2	204.07	239.83	228.59	273.89
K3	277.97	234.95	316.26	277.10
R	73.9	19.13	132.25	99.23

of concentration of SYD and dosage of AWAC on removal efficiency and adsorption capacity are obvious. The pH also had played an important role in the adsorption of SYD to AWAC. Temperature had the smallest effect on the adsorption rate and adsorption capacity.

4. Conclusions

In this work, AWAC was oxidized with phosphoric acid and evaluated for its ability to remove SYD from aqueous

solutions. The surface area of the activated carbon was relatively high (736.3 m²), and the AWAC structure was found to be a well-developed array of microvoids and mesopores, with an average pore size of 4.05 nm. An AWAC dose of 0.8 g/L displayed a high adsorption capacity (~96%) at an initial concentration of 150 mg/L of SYD. The maximum adsorption capacity (~271 mg/g) occurred at a temperature of 308 K. The influence of initial concentration of SYD, pH, temperature and dosage of AWAC have been studied. The adsorption experimental data fit well to the Langmuir equation at 298 K ($R^2 = 0.9992$), which indicates monolayer adsorption. The adsorption kinetics of sorbents fit a pseudo-second-order model, indicating the rate-limiting factor is bond formation between the SYD and AWAC. Thermodynamic studies revealed that the adsorption process is spontaneous and endothermic. FTIR revealed that there were abundant –OH, C=C, and C–O–C functional groups on the surface of the AWAC, which may increase the sorption. Electrostatic attraction, chemical bonding and hydrophobic interaction with surface functional groups were identified in the adsorption mechanisms for SYD removal.

Acknowledgments

This work was supported by the Promotional research fund for excellent young and middle-aged scientists of Shandong Province (No. BS2014HZ019), the China Postdoctoral Science Foundation (No. 2014M551950), A Project of Shandong Province Higher Educational Science and Technology Program (No. J15LE07 and No. J15LH06), Natural Science Foundation of Shandong Province (No. ZR2016DM09) and the Major Science and Technology Program for Water Pollution Control and Treatment (No. 2012ZX07203004, 2015ZX07203005 and 2015ZX07203-007-005).

References

- [1] P.K. Malik, Dye removal from wastewater using activated carbon developed from sawdust: adsorption equilibrium and kinetics, *J. Hazard. Mater.*, 113 (2004) 81–88.
- [2] M. Rafatullah, O. Sulaiman, R. Hashim, A. Ahmad, Adsorption of methylene blue on low-cost adsorbents: a review, *J. Hazard. Mater.*, 177 (2010) 70–80.
- [3] M. Ghaedi, A. Hekmati Jah, S. Khodadoust, R. Sahraei, A. Daneshfar, A. Mihandoost, M.K. Purkait, Cadmium telluride nanoparticles loaded on activated carbon as adsorbent for removal of sunset yellow, *Spectrochimica Acta. Part A, Mol. Biomol. Spectrosc.*, 90 (2012) 22–27.
- [4] F.P. de Sá, B.N. Cunha, L.M. Nunes, Effect of pH on the adsorption of Sunset Yellow FCF food dye into a layered double hydroxide (CaAl-LDH-NO₃), *Chem. Eng. J.*, 215–216 (2013) 122–127.
- [5] Q. Gao, H. Liu, C. Cheng, K. Li, J. Zhang, C. Zhang, Y. Li, Preparation and characterization of activated carbon from wool waste and the comparison of muffle furnace and microwave heating methods, *Powder. Technol.*, 249 (2013) 234–240.
- [6] S.S. Nawar, H.S. Doma, Removal of dyes from effluents using low-cost agricultural by-products, *Sci. Total. Environ.*, 79 (1989) 271–279.
- [7] M.H. Julien, B. Skarratt, G. Maywald, Potential geographical distribution of alligator weed and its biological control by *Agasicles hygrophila*, *J. Aquatic. Plant Manage.*, 33 (1995) 55–60.
- [8] X.S. Wang, Y.P. Tang, S.R. Tao, Kinetics, equilibrium and thermodynamic study on removal of Cr (VI) from aqueous solutions using low-cost adsorbent Alligator weed, *Chem. Eng. J.*, 148 (2009) 217–225.
- [9] W. Liu, J. Zhang, C. Zhang, L. Ren, Sorption of norfloxacin by lotus stalk-based activated carbon and iron-doped activated alumina: Mechanisms, isotherms and kinetics, *Chem. Eng. J.*, 171 (2011) 431–438.
- [10] Q.-S. Liu, T. Zheng, P. Wang, L. Guo, Preparation and characterization of activated carbon from bamboo by microwave-induced phosphoric acid activation, *Ind. Crop. Prod.*, 31 (2010) 233–238.
- [11] Q. Kong, Y.-N. Wang, L. Shu, M.-S. Miao, Isotherm, kinetic, and thermodynamic equations for cefalexin removal from liquids using activated carbon synthesized from loofah sponge, *Desal. Water Treat.*, 57 (2016) 7933–7942.
- [12] M.S. Miao, Q. Liu, L. Shu, Z. Wang, Y.Z. Liu, Q. Kong, Removal of cephalexin from effluent by activated carbon prepared from alligator weed: Kinetics, isotherms, and thermodynamic analyses, *Process Safe. Environ.* (2016) DOI: 10.1016/j.psep.2016.03.017.
- [13] N. Yalçın, V. Sevinc, Studies of the surface area and porosity of activated carbons prepared from rice husks, *Carbon*, 38 (2000) 1943–1945.
- [14] A. Shanmugaraj, J. Bae, K.Y. Lee, W.H. Noh, S.H. Lee, S.H. Ryu, Physical and chemical characteristics of multiwalled carbon nanotubes functionalized with aminosilane and its influence on the properties of natural rubber composites, *Compos. Sci. Technol.*, 67 (2007) 1813–1822.
- [15] J.T. Klopogge, D. Wharton, L. Hickey, R.L. Frost, Infrared and Raman study of interlayer anions CO₃²⁻, NO₃⁻, SO₄²⁻ and ClO₄⁻ in Mg/Al-hydrotalcite, *Am. Mineral.*, 87 (2002) 623–629.
- [16] M.S. Miao, X.D. Yao, L. Shu, Y.J. Yan, Z. Wang, N. Li, X.T. Cui, Y.M. Lin, Q. Kong, Mixotrophic growth and biochemical analysis of *Chlorella vulgaris* cultivated with synthetic domestic wastewater, *Int. Biodeter. Biodegr.*, 113 (2006) 120–125.
- [17] S.G. Pouloupoulos, M. Nikolaki, D. Karampetsos, C.J. Philippopoulos, Photochemical treatment of 2-chlorophenol aqueous solutions using ultraviolet radiation, hydrogen peroxide and photo-Fenton reaction, *J. Hazard. Mater.*, 153 (2008) 582–587.
- [18] R.J.D. Jonge, A.M. Breure, J.G.V. Andel, Reversibility of adsorption of aromatic compounds onto powdered activated carbon (PAC), *Water Res.*, 30 (1996) 883–892.
- [19] I. Tan, A. Ahmad, B. Hameed, Adsorption isotherms, kinetics, thermodynamics and desorption studies of 2, 4, 6-trichlorophenol on oil palm empty fruit bunch-based activated carbon, *J. Hazard. Mater.*, 164 (2009) 473–482.
- [20] J.F. Osuma, V. Saravia, J.L. Toca-Herrera, S.R. Couto, Sunflower seed shells: a novel and effective low-cost adsorbent for the removal of the diazo dye Reactive Black 5 from aqueous solutions, *J. Hazard. Mater.*, 147 (2007) 900–905.
- [21] A.M. Vargas, A.L. Cazetta, M.H. Kunita, T.L. Silva, V.C. Almeida, Adsorption of methylene blue on activated carbon produced from flamboyant pods (*Delonix regia*): Study of adsorption isotherms and kinetic models, *Chem. Engng. J.*, 168 (2011) 722–730.
- [22] D. Savova, N. Petrov, M.F. Yardim, E. Ekinici, T. Budinova, M. Razvigorova, V. Minkova, The influence of the texture and surface properties of carbon adsorbents obtained from biomass products on the adsorption of manganese ions from aqueous solution, *Carbon*, 41 (2003) 1897–1903.
- [23] M.-S. Miao, Y.-N. Wang, Q. Kong, L. Shu, Adsorption kinetics and optimum conditions for Cr(VI) removal by activated carbon prepared from luffa sponge, *Desal. Water. Treat.*, 57 (2016) 7763–7772.
- [24] W.J. Weber, J.C. Morris, Kinetics of adsorption on carbon from solution, *J. Sanit. Engin. Div.*, 89 (1963) 31–60.
- [25] S. Allen, G. McKay, K. Khader, Intraparticle diffusion of a basic dye during adsorption onto sphagnum peat, *Environ. Pollut.*, 56 (1989) 39–50.

- [26] I. Langmuir, The adsorption of gases on plane surfaces of glass, mica and platinum, *J. Am. Chem. Soc.*, 40 (1918) 1361–1403.
- [27] T.W. Weber, R.K. Chakravorti, Pore and solid diffusion models for fixed-bed adsorbers, *AIChE. J.*, 20 (1974) 228–238.
- [28] G. Cerofolini, A model which allows for the Freundlich and the Dubinin-Radushkevich adsorption isotherms, *Surf. Sci.*, 51 (1975) 333–335.
- [29] M. Ghaedi, A.H. Jah, S. Khodadoust, R. Sahraei, A. Daneshfar, A. Mihandoost, M. Purkait, Cadmium telluride nanoparticles loaded on activated carbon as adsorbent for removal of sunset yellow, *Mol. Biomol. Spectrosc.*, 90 (2012) 22–27.
- [30] M. Ghaedi, Comparison of cadmium hydroxide nanowires and silver nanoparticles loaded on activated carbon as new adsorbents for efficient removal of Sunset yellow: Kinetics and equilibrium study, *Mol. Biomol. Spectrosc.*, 94 (2012) 346–351.
- [31] M. Maghsoudi, M. Ghaedi, A. Zinali, A. Ghaedi, M. Habibi, Artificial neural network (ANN) method for modeling of sunset yellow dye adsorption using zinc oxide nanorods loaded on activated carbon: Kinetic and isotherm study, *Mol. Biomol. Spectrosc.*, 134 (2015) 1–9.
- [32] A.A. Khan, R. Singh, Adsorption thermodynamics of carbofuran on Sn (IV) arsenosilicate in H⁺, Na⁺ and Ca²⁺ forms, *Colloids. Surf.*, 24 (1987) 33–42.
- [33] İ.A. Şengil, M. Özacar, Biosorption of Cu (II) from aqueous solutions by mimosa tannin gel, *J. Hazard. Mater.*, 157 (2008) 277–285.
- [34] Z.-Z. Li, L.-X. Wen, L. Shao, J.-F. Chen, Fabrication of porous hollow silica nanoparticles and their applications in drug release control, *J. Control. Release*, 98 (2004) 245–254.